Bulletin of the American Meteorological Society

Volume 72 Number 1 January 1991

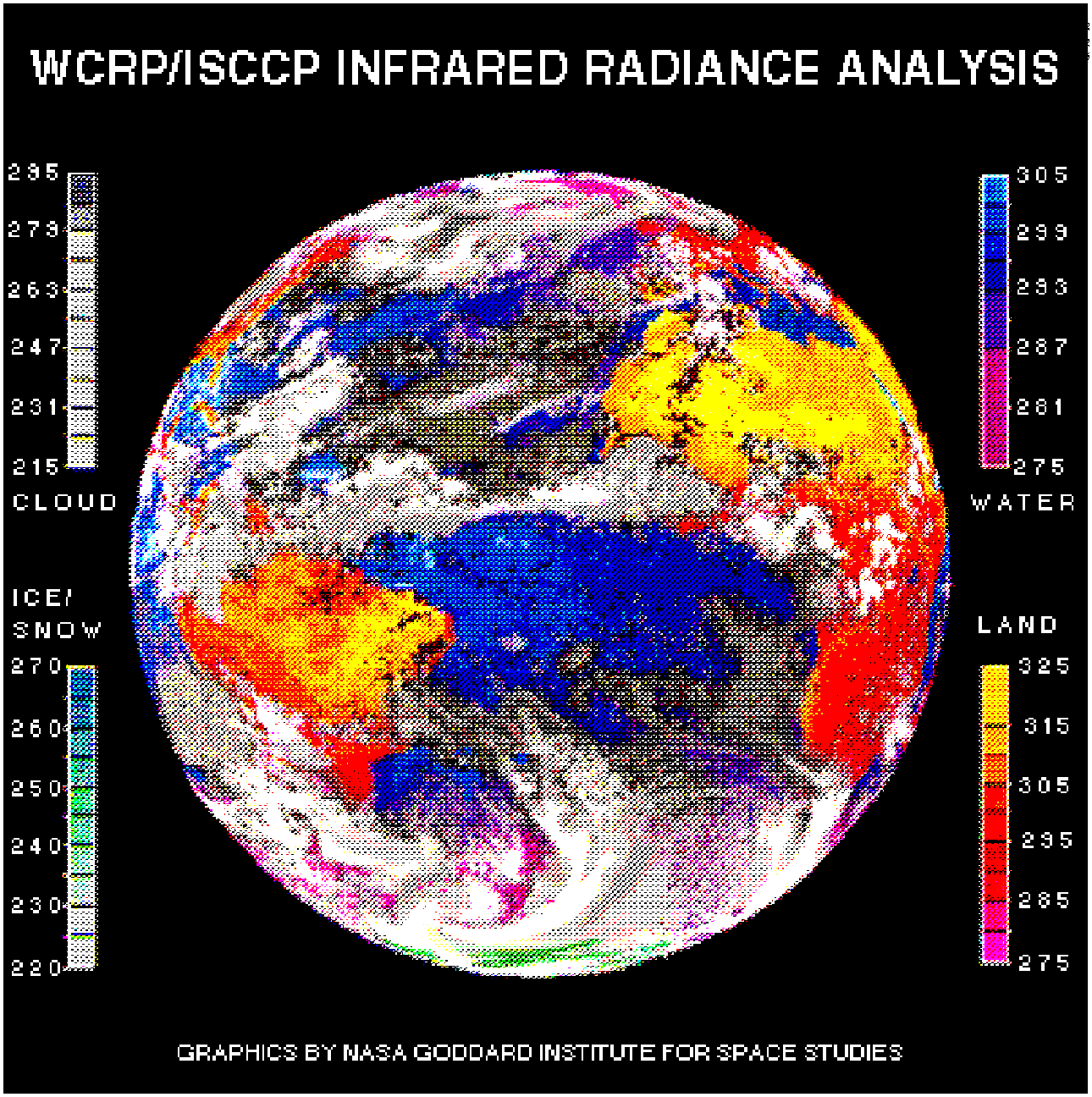

[Reprinted from BULLETIN OF THE AMERICAN METEOROLOGICAL SOCIETY, Vol. 72, No. 1, January 1991]
Printed in U.S.A.

ISCCP Cloud Data Products

William B. Rossow and
Robert A. Schiffer

Cover: Brightness temperature image of the earth on 4 July 1983 at 1500 UTC, as viewed by a hypothetical geostationary satellite at 25°W, synthesized from data taken by METEOSAT-2, GOES-5, and NOAA-7 for ISCCP. Application of different color tables representing the brightness temperatures of clear scenes over land, open water, or snow/ice and cloudy scenes depends on the ISCCP cloud detection analysis. Spatial resolution is approximately 55 km.

ISCCP Cloud Data Products

William B. Rossow* and
Robert A. Schiffer+

Abstract

The operational data collection phase of the International Satellite Cloud Climatology Project (ISCCP) began in July 1983. Since then, visible and infrared images from an international network of weather satellites have been routinely processed to produce a global cloud climatology. This report outlines the key steps in the data processing, describes the main features of the data products, and indicates how to obtain these data. We illustrate some early results of this analysis.

1. Project objectives and history

The complexity of the distribution and multi-scale variations of cloudiness and its interactions with the radiation coming from the sun and emitted by the earth's surface makes determining its role in the climate very challenging. Since clouds have first-order effects on radiation and water exchanges in the atmosphere, their role must be central. Since the dynamical motions that are forced by these same energy exchanges control the nature and distribution of clouds, clouds are involved in a crucial set of feedbacks on climate changes. The International Satellite Cloud Climatology Project (ISCCP) was established as part of the World Climate Research Program (WCRP) to:

a. produce a global, reduced-resolution, calibrated and normalized, infrared- and visible-radiance data set, along with basic information on the radiative properties of the atmosphere, from which cloud parameters can be derived;

b. coordinate basic research on techniques for inferring the physical properties of clouds from satellite radiance data;

c. derive and validate a global cloud climatology;

d. promote research using ISCCP data to improve parameterizations of clouds in climate models; and,

e. improve understanding of the earth's radiation budget (top-of-the-atmosphere and surface) and hydrological cycle (Schiffer and Rossow 1983).

The ISCCP is part of a strategic attack on these research problems that involves data and analysis results from a number of other projects as well (WCRP 1984a), including the Earth Radiation Budget Experiment (ERBE) (Barkstrom and Smith 1986), a Surface Radiation Budget project (SRB) (WCP 1986b), a Global Precipitation Climatology Project (GPCP) (WCP 1985), and a series of surface process studies in ISLSCP (WCRP 1984b). All of these individual efforts will be brought together in the Global Energy and Water Experiment (GEWEX) (WCP 1987).

Operational data collection and processing for ISCCP have been underway since July 1983. Resolution of many difficulties with the satellite radiance data and development of a comprehensive cloud algorithm and radiative transfer model has meant a gradual build-up of data production. All data processing centers[1], with the exception of a Sector Processing Center for INSAT data, are fully operational and all data products are being delivered to the central archives.

To obtain global coverage while resolving diurnal variations, the project planned on using data from at least one polar-orbiting and five geostationary weather satellites, although data from a second polar-orbiting satellite was desired (Schiffer and Rossow 1983). Planned collection was to last five years. Actual coverage, measured against this ideal, over the first six years is shown in Figure 1. Because of the loss of one polar-orbiting satellite, two GOES satellites, and two GMS satellites, coverage has averaged about 90% for only three out of six years. If INSAT data can be obtained and processed, then one year of data would exceed the originally sought coverage. This history is a rather graphic commentary on the feasibility of current plans for an improved earth observing satellite system. ISCCP data collection and processing has been extended through 1995 to continue producing data for other WCRP projects (WMO 1989). Prospects for coverage are somewhat

*NASA Goddard Institute for Space Studies, New York, NY 10025
+NASA Headquarters, Washington, DC 20546

[1]ISCCP Stage B3 data (reduced volume visible and infrared images) are produced from reduced resolution data supplied by the European Space Agency for METEOSAT, the Japanese Meteorological Agency for GMS, the Atmospheric Environmental Service of Canada for GOES-EAST (the University of Wisconsin also supplied GOES-EAST data), Colorado State University for GOES-WEST and the National Oceanographic and Atmospheric Administration for the polar-orbiters. METEOSAT, GMS, GOES-EAST, GOES-WEST, and INSAT refer to geostationary weather satellites; NOAA is used to refer to the polar-orbiting weather satellites. The Centre de Meterologie Spatiale at Lannion conducts the radiance normalization and the NASA Goddard Institute for Space Studies produces the final data products. All data products are archived by NOAA NESDIS in Washington, D.C.

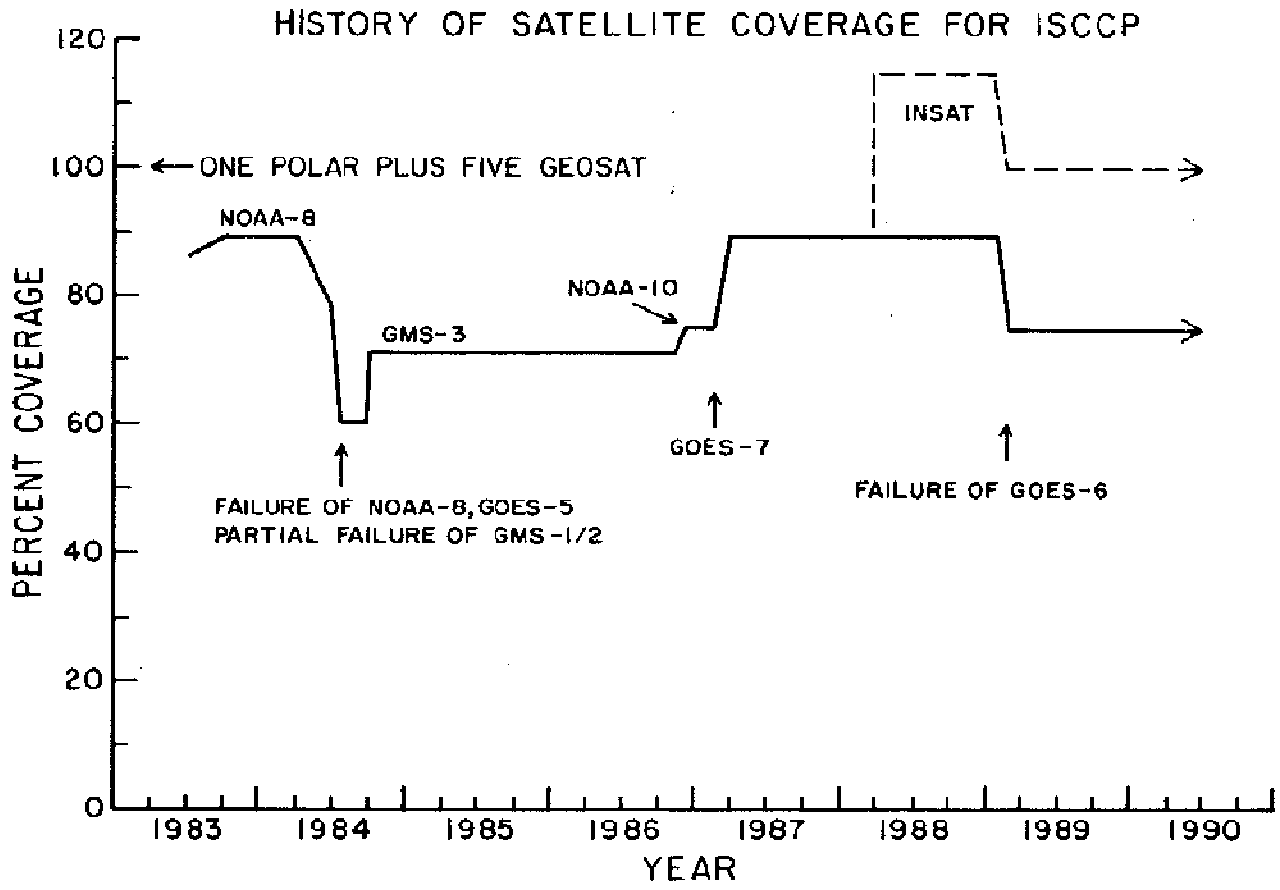

FIG. 1. History of weather satellite coverage for ISCCP. The coverage provided by five geostationary satellites and one polar orbiting satellite is defined arbitrarily to be 100%, representing eight observations per day at each location (the actual observation frequency is somewhat smaller near 50°-60° latitude. The initial complement of satellites was NOAA-7, METEOSAT-2, GMS-2, GOES-5 and GOES-6. Failures and replacements of satellites are indicated. Time is given in quarter years.

better: the next series of GOES satellites will begin in 1991 and arrangements for delivery of INSAT-2 data in 1991 are being made. The reduced volume radiance dataset (Stage B3) was described by Schiffer and Rossow (1985). This paper describes the two cloud climatology data products, Stages C1 and C2.

2. Datasets

One of the primary data products of ISCCP is a collection of visible (VIS) and infrared (IR) radiance[2] images from all of the operational weather satellites that have been placed into a common format and have been normalized to a standard reference calibration (Schiffer and Rossow 1985). These Stage B3 data are a reduced resolution version of the original images, produced by sampling in both time and space to a nominal spacing of 3 hr and 30 km (see cover figure). These data are the primary input for an analysis that produces the cloud climatology data (see detailed documentation of these data in Rossow et al. 1987).

Geographic data sets are used in the analysis to specify as a function of latitude/longitude the land/-water fraction (at a resolution of about 25 km), the mean topography (at a resolution of 25 km), and the surface/vegetation type (at a resolution of about 100 km). Daily atmospheric temperature profiles, humidity profiles and ozone column abundance are obtained from the TIROS Operational Vertical Sounder (TOVS) analysis product produced by NOAA. Weekly snow and sea ice cover are provided by operational analyses of NOAA and the U.S. Navy (see more details in Rossow et al. 1988).

The analysis results can only be used for climate studies if the radiance data have a common and constant calibration. Such a calibration has been established for the ISCCP data, based on four acti-

[2]If images at other wavelengths are also available, these are included in the ISCCP Stage B3 data, although normalization of their calibration has not been done.

vities. First, the ISCCP project conducts routine data comparisons between each geostationary satellite and the afternoon NOAA polar-orbiter, which normalizes all radiance measurements to a single satellite (Schiffer and Rossow 1985; Rossow et al. 1987). Second, the project normalizes the relative calibrations of all the afternoon (and morning) polar-orbiters to that of NOAA-7 in July 1983 and monitors them for long-term drifts during their lifetimes (Brest and Rossow 1990). Figure 2 shows the history of VIS and IR calibrations over the first five years of the project. The corrections that were required for the NOAA-9 visible radiances are shown in Fig. 2a. Figure 2b shows that the IR channel sensitivities vary with time, but that the operational calibration procedure generally corrects for these changes − only a small adjustment was required in late 1987 through 1988. Third, further statistical tests are applied by the project to detect short-term (two weeks) calibration anomalies, usually in the IR channels of the geostationary satellites. These short-term anomalies are also removed.

In addition, NASA is continuing a series of aircraft flights, begun by NOAA, to provide occasional measures of the absolute calibrations of the visible channels on the polar-orbiting satellites. The combination of the results from these flights, from several other independent efforts to calibrate the polar-orbiters, and from the ISCCP monitoring has established a comprehensive and well-documented absolute VIS calibration for NOAA-9 (Whitlock et al. 1990).

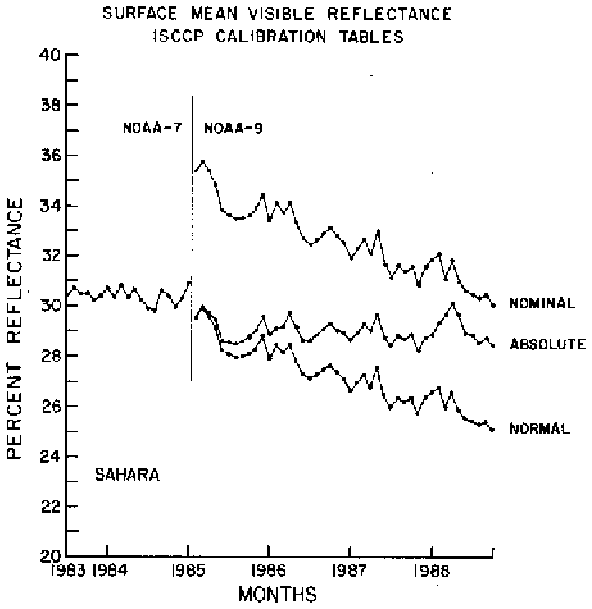

FIG. 2. History of the AVHRR (a) VIS (0.6 µm−Channel 1) and (b) IR (10.5 µm−Channel 4) calibrations for NOAA-7 and NOAA-9. The VIS calibration is illustrated by the monthly mean VIS reflectance averaged over the Sahara desert. The nominal calibration refers to the original supplied by the satellite operator (NOAA); the normalized calibration refers to that used to match NOAA-9 to NOAA-7 in January 1985. Absolute calibration refers to the final calibration after adjustment for instrument drift. The IR calibration is illustrated by showing the global, monthly mean IR counts and brightness temperatures. Although the NOAA-7 and NOAA-9 instrument counts differ and the NOAA-9 instrument count values drift over time, the calibrated brightness temperatures are nearly constant when averaged over the seasonal cycle. A small correction is made in late 1987 and 1988. Time is given in months.

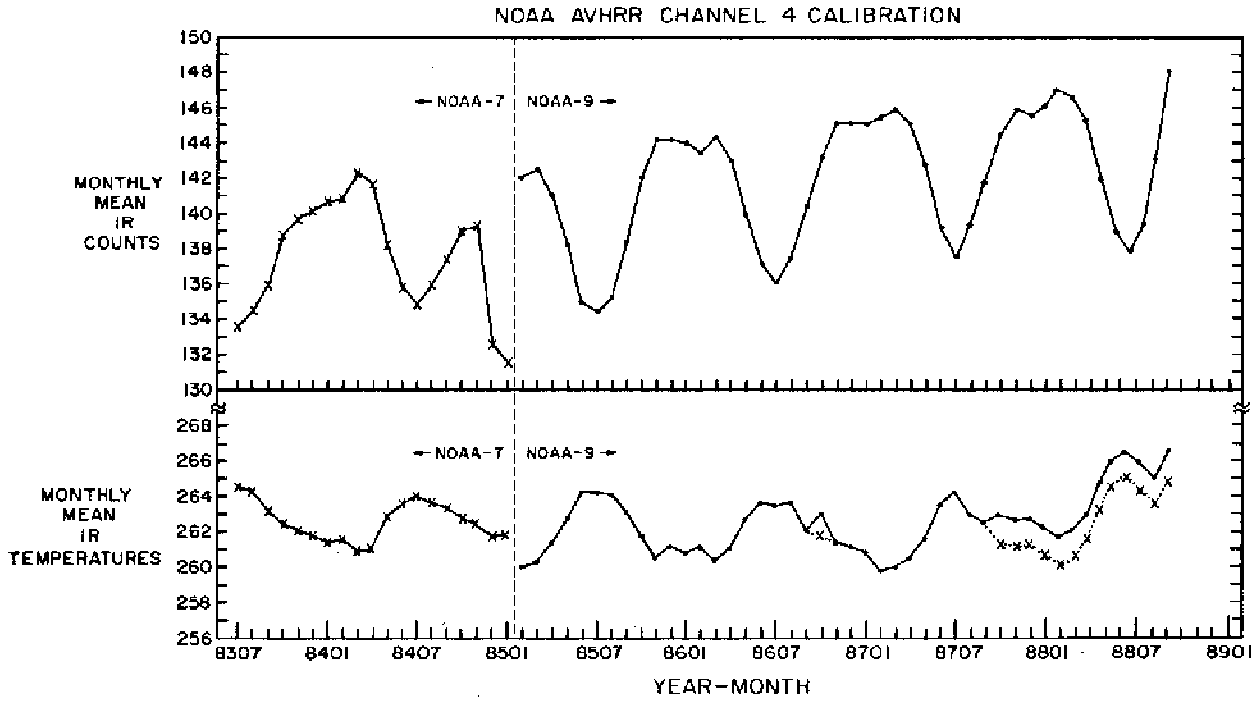

The initial ISCCP VIS radiance calibration was that of NOAA-7 AVHRR Channel 1, as measured in July 1983 (Rossow et al. 1987); but the uncertainties in this calibration were large. All ISCCP Stage B3 VIS radiances are still reported with this calibration. To place these data into the same calibration as established for NOAA-9 requires multiplying all visible radiance values from ISCCP B3 data tapes by 1.2. This change in the VIS calibration is made before the ISCCP cloud analysis is done. The IR calibration remains that of the original NOAA-7 AVHRR calibration.

3. Cloud analysis procedure

The ISCCP cloud analysis procedure has three principal parts: cloud detection, radiative model analysis, and statistical analysis (Rossow et al. 1988). Cloud detection refers to the separation of the image pixels[3] into cloudy and clear scenes. This process is performed by what is often referred to as a "cloud algorithm"; intercomparisons of several existing cloud algorithms were conducted to facilitate the design of a global analysis method (Rossow et al. 1985). Each scene is then compared to calculations of a radiative transfer model that simulates the radiances that should be measured by the satellites as a function of surface visible reflectance and temperature (clear scenes) and cloud optical thickness and cloud top temperature (cloudy scenes). The effects of the atmosphere on the radiances are accounted for using the TOVS data for each location and time. All the results from each satellite are reduced to a spatial resolution of about 280 km by collecting statistics (mean, standard deviation and frequency distributions) of the spatial variability of the surface and clouds and by merging the results from all the satellites. These data are called the Stage C1 data, which report global results every three hours (see Table 1 for a list of contents). Monthly averages of the C1 data are also produced, called Stage C2 data (see Table 2).

This cloud analysis is considered to be experi mental, though state-of-the-art; hence, the strategy is to report more about the results than the "answer". The cloud detection procedure is an inherently statistical decision process, in that all the attributes used to make the decision are obtained from the distribution of radiances over space and time. Therefore, the results are expected to be "correct" only in a statistical sense, though the errors at any one place and time are estimated and reported in the data. In addition to uncertainties in the detection, there are uncertainties in the interpretation of the radiances (see Rossow 1989). The most important of these is the assumption that all image pixels containing cloud are

TABLE 1: C1 Data Contents

Global information provided every 3 h for each 280 km grid cell
Cloud amount and distribution information
Total number of image pixels
Total number of cloudy pixels
Total number of IR-cloudy pixels
Total number of marginal cloudy pixels
Total number of IR-only cloudy pixels
Number of cloudy pixels in 7 PC classes
Number of cloudy pixels in 35 PC/TAU classes
Average total cloud properties
PC, cloud top pressure without visible channel information
PC, cloud top pressure with visible channel information
PC, cloud top pressure of marginal clouds
Spatial variation of PC
TC, cloud top pressure without visible channel information
TC, cloud top pressure with visible channel information
TC, cloud top pressure of marginal clouds
Spatial variation of TC
TAU, cloud optical thickness
TAU, cloud optical thickness of marginal clouds
Spatial variation of TAU
Average surface properties
PS, surface pressure
TS, surface temperature
RS, surface visible reflectance
Snow/ice cover fraction
Topography and land/water flag
Average radiances
IR-cloudy
IR-clear
Spatial variation of IR
VIS-cloudy
VIS-clear
Spatial variation of VIS
Viewing geometry and day/night flag
Satellite identification
Average atmospheric properties
T, atmospheric temperatures for seven levels
TS, surface temperature
TT, tropopause temperature
PT, tropopause pressure
PW, precipitable water amount for five levels
O3, column ozone abundance
Source of atmospheric data

[3]Each image pixel is about 4-8 km in size, but the Stage B3 data have been sampled to a pixel spacing of about 30 km. Because of navigation uncertainties, the pixel location is not more precise than about 30 km and is variable within this range. Hence, in the cloud analysis, each image pixel is treated as representing a specific scene about 30 km across, referred to as a B3 data pixel.

completely covered by a single, homogeneous layer. We do not have a better scheme yet, but we have tried to preserve enough additional information to allow for later improvement of the results.

a. Cloud detection

The cloud detection step examines all of the B3 radiance data for one month to collect statistics on the space/time variations of the VIS and IR radiances. The key assumptions used in the analysis are that the radiances in clear scenes are less variable than in cloudy scenes and that it is the clear scenes that compose the "darker" and "warmer" parts of the VIS and IR radiance distributions, respectively (cf., Rossow et al. 1985; Rossow et al. 1989b; Sèze and Rossow 1990). Based on these statistics, estimates are made of the clear values of VIS and IR for each location and time. The maps of these values are referred to as the "clear sky composites". This approach is novel in two respects. First, all of the tests usually used to detect cloudiness directly, many of which were first proposed by other investigators (cf., Rossow et al. 1989b for a review), are here used to eliminate clouds to find clear scenes. There are two advantages. The tests can be stricter, because only an estimate of clear radiances is required, not a decision in each image at each location. In other words, not all clear scenes need to be found, only enough for a reliable estimate of clear radiances. The second advantage is that the cloud detections can be directly validated by comparing the clear radiances, which are dominated by the surface properties, to other measurements of the surface properties. The second novel aspect is the use of time variations at one location to detect cloudiness (cf. Desbois and Sèze 1984; Rossow et al. 1985; Gutman et al. 1987; Sèze and Desbois 1987).

After estimates of clear radiances are obtained for each place and time, the entire B3 radiance data set is examined again to compare each radiance value to its corresponding clear value. The differences are compared to the uncertainties in estimating the clear radiances: if the differences are larger than the uncertainty and in the "cloudy direction" at either wavelength (colder IR or brighter VIS), then the pixel is labeled cloudy. In fact, each pixel is labeled to indicate the position of its radiance values relative to the clear values according to the scheme illustrated in Figure 3. The radiance plane is divided by intervals that represent the magnitude of the uncertainty in the clear radiances; the lower and upper ranges extend all the way to the minimum and maximum possible values.

Since the precise value of the threshold (magnitude of clear radiance uncertainty) is also uncertain, one estimate of the error in the identification is given by counting the frequency of radiance values that are "close" to the dividing line between the clear and cloudy categories. These pixels are defined by threshold flag values of 4 in both channels (Fig. 3). We refer to these pixels as "marginally cloudy", since they are just barely detected. This category includes some thin cirrus clouds and low-level broken cloudiness (more low-level cloudiness is included in this category at night when only IR data are available). We believe that these "marginal clouds" are actually clouds, since we set the thresholds to the uncertainty in the clear radiances; i.e., this approach avoids spurious detec-

TABLE 2: C2 Data Contents

Global, monthly average information provided at eight times of day and over all times of day
Cloud amount information
Monthly average cloud amount
Monthly frequency of cloud occurrence
Monthly average IR-cloud amount
Monthly average marginal cloud amount
Average total cloud properties
PC, cloud top pressure
Average spatial and temporal variations of PC
TC, cloud top temperature
Average spatial and temporal variations of TC
TAU, cloud optical thickness
Average spatial and temporal variations of TAU
ALB, cloud spherical albedo
Average spatial and temporal variations of ALB
Average properties (amount, PC, TC, TAU) for cloud types
Low cloud (IR-only)
Middle cloud (IR-only)
High cloud (IR-only)
Cumulus, stratocumulus cloud
Stratus cloud
Alto-cumulus, alto-stratus cloud
Nimbostratus cloud
Cirrus cloud
Cirro-cumulus, cirro-stratus cloud
Deep convective cloud
Average surface properties
TS, surface temperature
Average temporal variations of TS
RS, surface visible reflectance
Snow/ice cover fraction
Average atmospheric properties
PS, surface pressure
TS, surface temperature
T5, temperature at 500 mb
PT, tropopause pressure
TT, tropopause temperature
ST, stratospheric temperature
PW, column water amount
O3, column ozone amount

tions of clouds, but misses some clouds. However, the interpretation of these clouds is uncertain, because partial coverage of the radiometer field-of-view can lead to intermediate radiance values that are arbitrarily close to the clear radiance values. Hence, the frequency of these "marginal clouds" may also be used to correct for resolution-dependent effects on the cloud amount.

b. Radiative analysis

Once each pixel is classified as clear or cloudy, the measured radiances can be compared to radiative transfer model calculations that include the effects of the atmosphere, surface and clouds. The attributes of the atmosphere, surface and clouds are represented in the model by a large number of physical properties (Rossow et al. 1988); but the availability of correlative data sets and restriction of the satellite radiances to two wavelengths limit the number of parameters that can be determined from the observations. The analysis strategy used exploits the correlative data to isolate the cloud effects and attributes all remaining radiance variation to changes in two cloud properties; other parameters are assigned climatological average values.

For VIS (0.6 μm) and IR (11 μm) wavelengths, atmospheric effects are small and depend on ozone and water abundances, the temperature profile and aerosol optical thickness. Complete information on ozone, water and temperature can be obtained from correlative data. Since little information is available concerning aerosol properties, their effects are neglected; however, since most aerosol occurs near the surface[4] and affects the upwelling radiation from there, our use of surface properties obtained from clear radiances with the same radiative model effectively incorporates the primary aerosol effects into these surface properties. The two surface properties retrieved from clear radiance values are the "visible" reflectance and the "brightness" temperature. The visible reflectance represents the amount of sunlight reflected by the surface at 0.6 μm and at a particular sun and satellite geometry (the view/illumination geometry is recorded in the data). Since most surfaces reflect sunlight anisotropically, the reflectance varies with satellite position, time of day and season. The temperature values correctly describe the IR radiances at the surface but are not equal to the actual physical temperature since most surfaces have IR emissivities slightly less than one. Little information exists concerning emissivities for land and vegetated surfaces, so all temperatures are retrieved assuming an emissivity of one.

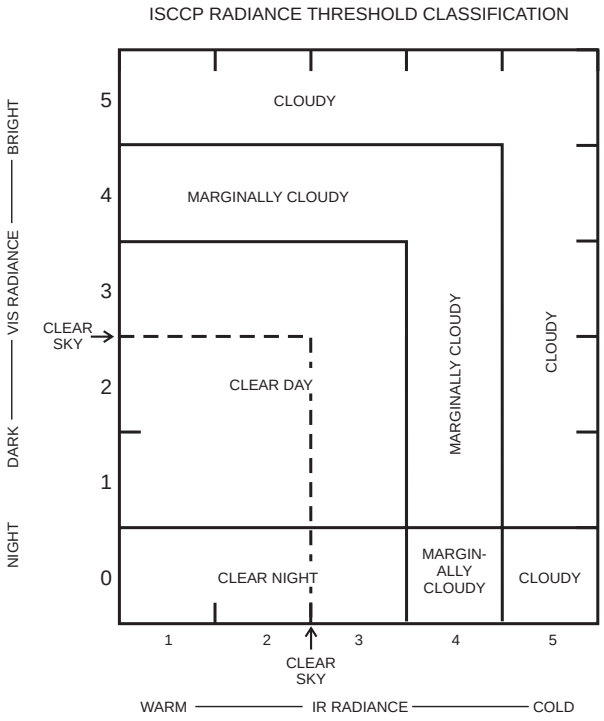

FIG. 3. Radiance threshold classification scheme applied to each satellite image pixel. The analysis determines a clear VIS and IR radiance value for each time and location, represented by the dashed lines. Each image pixel is then classified by the distance of its VIS and IR radiances from these clear values. The radiance intervals, 2, 3 and 4, on each axis are equal to the VIS and IR threshold values (3% and 2.5K for water regions and 6% and 6K for land regions, respectively).

Clouds are represented in the model as a single, thin (i.e., isothermal) layer, uniformly covering the image pixel and composed of water droplets with a specified average size (10 μm) and size distribution. All variations of cloudy radiances are attributed to changes in "visible" optical thickness (defined at 0.6 μm) and a temperature. The optical thickness para meter determines the amount and angular distribution of sunlight reflected by the cloud layer (the full effects of multiple scattering are included) and the temperature is a "brightness" temperature, like that for the surface, that is interpreted to represent the physical temperature at the top of an opaque cloud layer. At night when only IR radiances are measured, no cloud optical thickness is reported and IR variations are associated with the cloud top "brightness" temperature. During the day, the cloud optical thickness value is related to an IR optical thickness in the model to correct for cloud emissivities less than one; both the original (opaque cloud value) and corrected cloud top temperatures are reported.

Other cloud properties may vary, including particle size, phase (water or ice), and size distribution (cf.

[4]Except after a large volcanic eruption. Large dust storms are generally detected as "clouds" and their properties retrieved as those of a water cloud.

Arking and Childs 1985). Moreover, vertical (subpixel-sized) and horizontal inhomogeneities, such as multiple layering or small scale "brokenness," can affect the radiances. If the role of these other cloud properties can be formulated (cf. Stephens 1988) and their value measured, then the retrieved optical thickness and temperature parameters in the ISCCP data set can be corrected by comparing the radiative model radiances calculated with and without the variation of these additional parameters to produce a transformation from one model to the other.

c. Statistics

The basic detection and radiative analysis is performed for each image pixel (see footnote page 3), producing detail like that illustrated by the cover figure. However, the cloud climatology data need to be reduced to a more manageable volume. This reduction requires that the spatial distribution of the pixel values be summarized in the Stage C1 data. This is done by projecting the pixel data into a standard map grid (resolution about 280 km) and calculating the average values of cloud and surface properties, as well as their standard deviations. To maintain approximately equal statistical significance, the map grid is an equal-area grid (cf., Rossow and Garder 1984). In addition, the explicit distributions of cloud optical thicknesses and top pressures (obtained from the top temperature and the atmospheric temperature profile) are reported (see fig. 4). All of these statistics are first collected for each satellite separately.

The final C1 data sets (one for each 3-h interval in a month) are assembled by "merging" the results from all the satellites. To preserve the statistical character and uniformity of the C1 results, "merging" is done by selection; i.e., only one result is reported for each map grid cell and any other results are discarded. The choice between satellites is made on the basis of two criteria: 1) a strong preference for time records produced from a single satellite and 2) limiting the satellite zenith angle (which also affects the number of pixels available). At low latitudes, the data reported generally come from the nearest geostationary satellite; if the primary data are missing then they are replaced by an adjacent geostationary satellite (if the zenith angle is not too large) or a polar-orbiter (if available at that time). In the polar regions, coverage is provided solely by the polar-orbiters, with the "afternoon" satellite preferred if two are available.

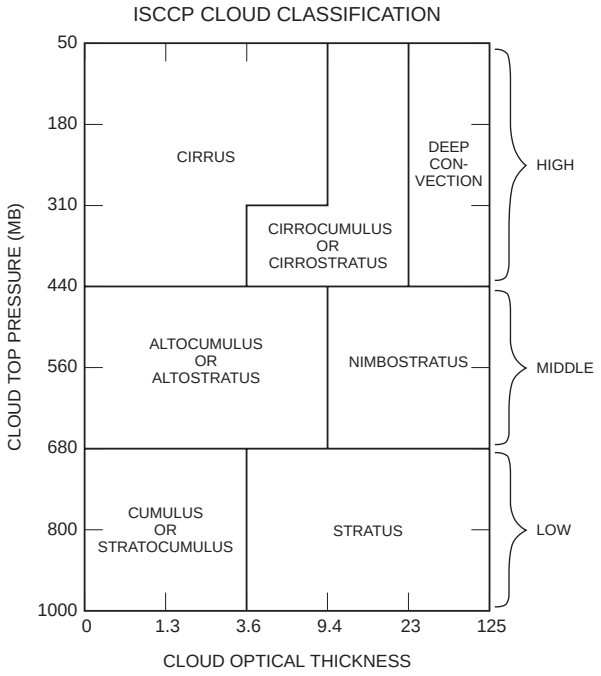

FIG. 4. Radiometric classification of cloudy pixels by the measured values of optical thickness and cloud top pressure (at night only cloud top pressures are determined, so that only the low, middle and high cloud types are counted). The frequency of cloudy pixels is reported in Stage C1 data for all thirty-five combinations of optical thickness and cloud top pressure intervals, indicated by the values on the axes. The association of classical morphological cloud type names with these ranges of cloud top pressure and optical thickness is only qualitative, but indicates the cloud types summarized in Stage C2.

4. Contents of data products

a. Stage C1 data

Stage C1 data represent a summary of the cloud analysis of every Stage B3 image pixel (VIS and IR radiances) at a spatial resolution of about 280 km. Pixel level data are collected into an equal-area map grid which has constant 2.5° latitude increments and variable longitude increments, ranging from 2.5° at the equator to 120° at the pole.

Each C1 data file represents all the available results within sequential three-hour periods; eight such periods cover each day, centered on 0, 3, 6, 9, 12, 15, 18 and 21 hours UTC. Data are organized onto two data tapes for each calendar month, 24 data tapes (6250 bpi density) per year.

The data are presented as 132 coded parameter values for each map grid cell; all values are given for each cell in turn. Table 1 lists the parameters[5]; more details can be found in the data documentation (Rossow et al. 1988).

[5]Symbols are: IR = infrared radiance (as a brightness temperature), VIS = visible radiance, PC = cloud top pressure, TC = cloud top temperature, TAU = cloud optical thickness, ALB = cloud albedo, PS = surface pressure, TS = surface temperature, RS = surface visible reflectance, T = atmospheric temperature (T5 = temperature at 500 mb), TT = tropopause temperature, PT = tropopause pressure, ST = stratosphere temperature at 15 mb, PW = precipitable water amount, and O3 = ozone abundance.

Cloud amount is reported by giving the total number of image pixels in the map grid cell and the total number of cloudy pixels present. All other "amounts" are reported as pixel numbers for better precision. In addition to the total cloud amount, which is determined by both the VIS and IR during the day and by IR-only at night, the C1 data contains a number of other "cloud amounts" to allow evaluation of the results (see Fig. 3). For diurnal studies, an IR-only cloud amount is also reported during the day for comparison to the nighttime results. The marginal cloud amounts (Fig. 3) indicate the sensitivity of the results to the magnitude of the radiance threshold. The distribution of the optical thicknesses and cloud top pressures for all the cloudy pixels in the grid cell are also given (Fig. 4), including a top pressure distribution determined solely from IR data for diurnal studies.

Cloud and surface properties are averaged over the corresponding pixels (cloudy and clear); the standard deviations of these values are also given. If a particular map grid cell is completely cloud covered, then no surface properties are reported; if the grid cell is completely clear, then no cloud properties are reported. However, the surface properties are also retrieved from the clear radiance composite values used to detect clouds; these values are always reported.

The average and standard deviations of the associated cloudy and clear radiances are given to allow comparative radiative studies that do not rely on the ISCCP radiative model assumptions. The viewing and illumination geometry are also reported.

The average properties of the marginal clouds are reported so that the effects of changing the magnitude of the radiance thresholds can be estimated. This allows for direct estimates of errors to the extent that the marginal cloud amount can be used as one estimate of cloud detection error.

The atmospheric temperature, water vapor profile and ozone abundance from the TOVS product produced by NOAA are reported, together with the snow/ice cover fraction obtained from the joint Navy/-NOAA operational products.

b. Stage C2 data

The Stage C2 data represent a monthly summary of the Stage C1 data. Average cloud, surface and atmospheric properties are given. Monthly averages are first made at constant diurnal phase for each of the three-hour periods; eight sets of averages for each month describe the mean diurnal variations of cloud and surface properties. The complete monthly mean is then constructed by averaging these eight sets. All nine averages are included in C2 data. In addition to reporting the time-mean of the spatial average and standard deviation, the time deviations of the C1 values are also given.

The distribution of cloud properties is summarized by reporting the average properties of ten cloud types (see Fig. 4): low, middle and high clouds defined by IR-only, cirrus, cirro-cumulus/stratus, convective clouds (optically thin, medium and thick high clouds), alto-cumulus/stratus and nimbostratus clouds (optically thin and thick middle clouds), and cumulus/-stratocumulus and stratus clouds (optically thin and thick low clouds). The first three types are defined solely by cloud top pressures, obtained from analysis of IR data only with no corrections for variable emissivities, and give the diurnal variations of the vertical distribution of cloudiness. The remaining seven cloud types are defined during daytime only by specific combinations of optical thickness and cloud top pressure. The combinations shown in Fig. 4 were selected primarily to differentiate among several types of clouds with different radiative feedbacks; however, some correspondence is also apparent with the classical dynamical cloud types reflected in the names. These results provide an accurate description of the variations of the distribution of clouds observed from satellites; but, since the classification is somewhat arbitrary, these results cannot necessarily be interpreted as a proper description of the morphological cloud types which have the same names.

Table 2 lists the parameters reported in Stage C2 data. One 6250 bpi density data tape can hold about two years of C2 data.

5. Some initial results

a. Validation

Validation of the ISCCP data products will involve comparisons to other measurements of the same or related cloud and surface properties and more detailed evaluations in special regional experiments (WCP 1986a). The regional studies will not only check the cloud radiative model used in the ISCCP analysis, but also assess the significance of other cloud properties not currently measured by satellites. In addition, use of the ISCCP data to diagnose cloud processes and verify climate model simulations will determine whether the measurement errors are acceptable or must be reduced by an improved analysis. We show only two examples of validation results as illustration.

Validation of the ISCCP cloud analysis involves three distinct issues: cloud detection, cloud amount determination, and retrieval of cloud radiative properties (cf., Rossow et al. 1989b). The first issue concerns whether the radiance data have been properly separated into parts that provide measures of

clear and cloudy conditions. The former can be used to measure surface optical properties (upon removal of atmospheric effects) and to represent the surface effects in an analysis of the latter. This most fundamental step in the analysis can be validated by confirming the accuracy of the clear radiances or surface properties retrieved from them: the cloud detection is considered "correct" if the actual clear radiances are found to lie within the range defined by the inferred values plus or minus the threshold magnitude.

One of the most straightforward checks of the clear IR radiances is to compare the retrieved sea surface temperatures (SST) to other measurements (cf., Rossow et al. 1989a). This tests not only the validity of the clear IR radiances, but also the radiative model calculation of water vapor absorption. Figure 5 shows the distribution of differences between the monthly mean SST for July 1983 from the Blended Analysis of ship, buoy and satellite data (Reynolds 1988) and the ISCCP surface brightness temperatures over ocean, where we subtract two monthly mean maps with 2.5° grid resolution and exclude near-coastal and sea-ice covered regions. The bias is nearly zero when higher satellite zenith angle data are excluded and the ISCCP values are only about 0.5K lower when they are included. Using the correct value of water emissivity makes the ISCCP SST values about 0.5 K warmer than the Blended Analysis values. There are a number of other factors that can change the bias estimate, including the difference between the sub-surface temperature measurements of ships and buoys and the surface "skin" measurement of satellite radiometers (Wright 1986; Schluessel et al. 1987; Karl et al. 1989) and changes in satellite radiometer calibration. Differences of up to 1 K can be explained by the different measurement systems (cf., Karl et al. 1989). The small increase in bias when data with larger satellite zenith angles are included suggests an underestimate of tropical water abundance by TOVS; this is consistent with the results of comparing TOVS water vapor abundances with those obtained by Oort (1988). Comparison of these two data sets in other months suggests variations of the bias of 0.5−1.0. K, consistent with calibration uncertainties (Brest and Rossow 1990). These sources of bias do not affect the cloud detection, however.

The variable component of the differences, which can affect the cloud detection, is about 2.5 K. Since the Blended Analysis results have an estimated uncertainty of about 1 K and uncertainties in water vapor abundances increase the uncertainty of the ISCCP values, Fig. 5 suggests that the uncertainty of the ISCCP clear IR radiances is certainly less than the assumed value of 2.5 K. Although differences between the ISCCP and Blended Analysis SST values are somewhat larger in a few specific regions with

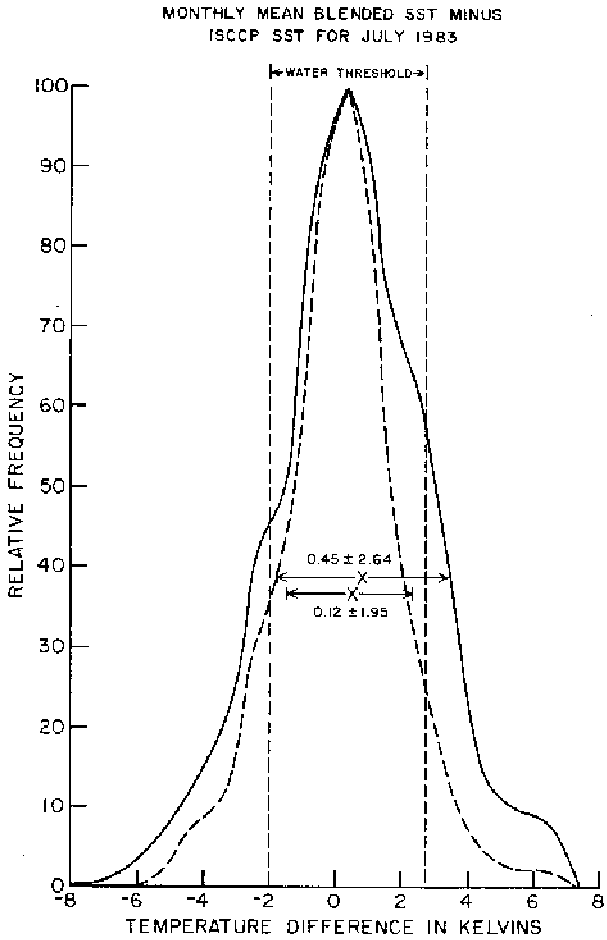

FIG. 5. Distribution of differences between maps of monthly mean ocean surface temperatures from a Blended Analysis of satellite and ship/buoy measurements (Reynolds 1988) and brightness temperatures retrieved from ISCCP clear IR radiances. The histogram summarizes the relative frequency of differences between two monthly mean maps with 2.5° grid resolution. Near-coastal and sea ice covered regions have been excluded. The dashed curve shows the effects of removing retrievals at higher satellite zenith angles (cosine < 0.6) from the comparison. The mean difference and the standard deviation are shown, together with the IR threshold employed to detect clouds over oceans.

very persistent cloud cover, use of an IR threshold of 2.5 K over oceans in the ISCCP cloud detection algorithm seems appropriate.

The second validation issue concerns not only the assignment of some cloud amount based on the number of satellite image pixels found to contain clouds, but also the proper representation of a cloudy atmosphere in radiative calculations (Stephens 1988; Rossow 1989). In the ISCCP analysis, all cloudy image pixels are treated as completely cloud covered. This assumption is coupled with the assumption in the radiative model analysis that the optical properties of cloudy air can be represented as homogeneous at the scale of the satellite image pixels (about 4-8 km), which in turn, determines the meaning of the

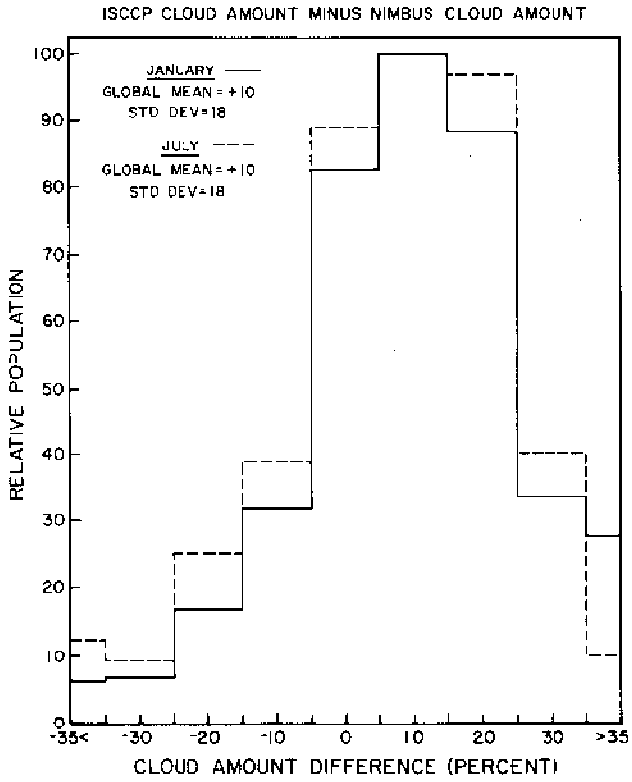

FIG. 6. Distribution of differences between maps of monthly mean cloud amounts determined by ISCCP and by the analysis of the NIMBUS-7 THIR/TOMS data set (Stowe et al. 1988, 1989) for January 1984 (solid) and July 1983 (dashed). The histogram summarizes the relative frequency of differences for maps with a 2.5° grid resolution. Mean differences and standard deviations are also given.

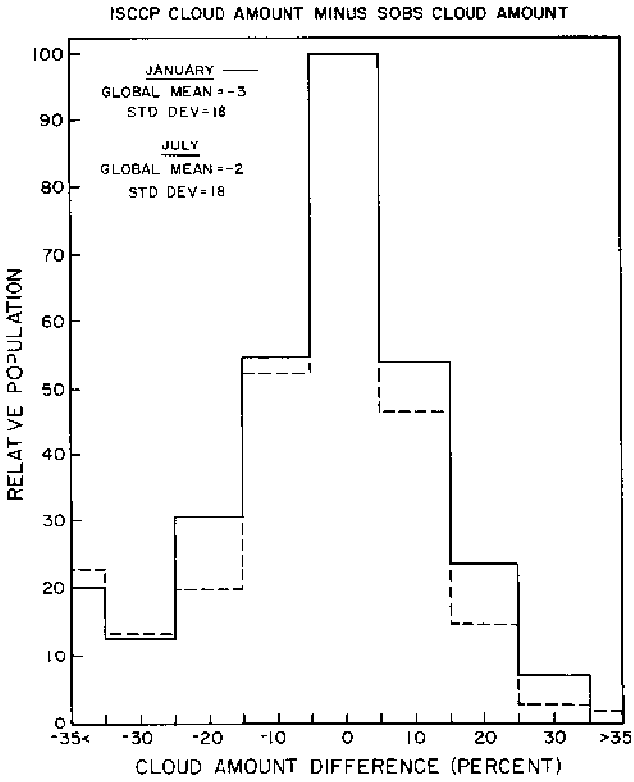

FIG. 7. Same as Fig. 6 but for differences between cloud amounts determined by ISCCP and by the analysis of SOBS (surface observations) (Warren et al. 1986; 1988) for January (solid) and July (dashed). ISCCP data are averaged over 1984–1985, whereas SOBS data are averaged over 1971–1981.

remaining cloud optical properties retrieved. Other assumptions about the smaller scale variations of clouds would produce a different coupling of the cloud amount and the optical properties; however, we do not have either a better assumption than this nor radiative models that can account for these smaller scale variations. Special regional experiments, such as FIRE (Cox et al. 1987), can improve understanding of this aspect of the problem. Note that this approach does properly represent the variations of clouds at scales larger than the image pixels; in fact, the monthly statistics of the variations in the spatially and temporally sampled ISCCP data have been shown to capture most of the same information as the original full resolution images (Sèze and Rossow 1990).

As a second example of validation, we compare the ISCCP cloud amounts to two other cloud climatologies (see discussion in Rossow et al. 1989b). Figure 6 shows the distribution of differences between the monthly mean cloud amounts reported by ISCCP and the NIMBUS-7 THIR/TOMS analysis (Stowe et al. 1988, 1989) for July 1983 and January 1984. Figure 7 shows the differences between the ISCCP results averaged over January 1984 and 1985 and July 1984 and 1985 and the cloud climatology collected from conventional surface weather observations (Warren et al. 1985; Warren et al. 1986; 1988), where the latter is an average over ten July's and January's from 1971 to 1981. The first comparison shows a bias between the two satellite climatologies, with the ISCCP global cloud amount about 10% higher than that of NIMBUS-7 (already noted in Stowe et al. 1989); whereas, the ISCCP results are biased only a few percent lower than the surface observations.

This comparison involves a number of complex issues concerning the definition of cloud amount, geometry differences, diurnal sampling differences, and analysis sensitivities. For example, examination of the regional distribution of these differences shows that the majority of the ISCCP-NIMBUS-7 difference occurs over the oceans, especially in the marine stratus regimes, and can be explained by the much smaller IR threshold employed by the ISCCP analysis. If the ISCCP results are modified to use a threshold closer to that used in the NIMBUS analysis, then the disagreements are reduced to less than 5% with a more

Table 3: Global, monthly mean cloud and surface properties

Month	Year	Cloud Amount (%)	Top Temperature (K)	Top Pressure (mb)	Optical Thickness	Surface Temperature (K)	Surface Reflectance (%)
Jul	83	58.8	271.8	673	10.3 (6.2)	291.3	15
Aug	83	59.0	272.0	677	9.6 (6.0)	291.3	14
Sep	83	58.5	271.8	678	9.1 (5.4)	291.5	13
Oct	83	59.2	270.1	675	10.0 (5.9)	288.9	15
Nov	83	58.9	269.6	673	11.2 (6.3)	287.8	17
Dec	83	58.6	269.1	671	10.7 (6.2)	287.0	17
Jan	84	57.6	269.1	676	10.1 (5.9)	287.2	16
Feb	84	58.7	269.8	673	9.5 (5.7)	288.6	14
Mar	84	59.6	270.0	683	9.5 (5.4)	289.0	15
Apr	84	58.9	270.7	683	9.8 (5.4)	290.2	15
May	84	58.6	270.5	678	11.2 (6.0)	289.9	17
Jun	84	57.6	272.0	690	10.4 (6.2)	290.6	16
Jul	84	58.7	272.0	686	8.9 (5.8)	291.6	14
Aug	84	57.4	271.5	686	8.8 (5.6)	291.6	14
Sep	84	58.3	270.8	676	8.1 (5.0)	290.7	12
Oct	84	60.6	270.2	669	8.8 (5.2)	290.6	12
Nov	84	59.9	270.0	672	8.6 (5.4)	289.8	14
Dec	84	61.2	269.4	670	9.6 (5.6)	288.9	14
Jan	85	60.2	269.6	678	9.1 (5.2)	288.8	14
Feb	85	60.4	267.8	656	9.4 (5.2)	287.8	15
Mar	85	61.8	268.9	669	9.2 (5.0)	289.6	15
Apr	85	61.5	270.1	675	8.6 (4.7)	291.5	15
May	85	60.4	270.1	671	8.5 (4.7)	291.2	15
Jun	85	59.1	270.6	671	8.0 (4.8)	291.5	15
Jul	85	60.0	270.9	669	7.0 (4.7)	291.8	13
Aug	85	60.0	271.3	675	7.5 (4.8)	292.4	13
Sep	85	59.7	270.9	675	7.4 (4.6)	291.6	12
Oct	85	60.5	270.1	671	8.6 (5.0)	290.3	13
Nov	85	61.8	269.3	668	9.1 (5.2)	289.5	15
Dec	85	61.0	269.0	670	9.1 (5.2)	288.8	15
Jan	86	60.7	269.3	671	8.4 (5.0)	289.1	14
Feb	86	59.7	269.3	679	8.6 (4.8)	288.9	14
Mar	86	61.1	269.8	674	7.9 (4.6)	290.0	14
Apr	86	61.8	269.4	671	8.1 (4.4)	290.2	15
May	86	60.9	270.1	679	8.4 (4.6)	291.4	15
Jun	86	60.9	270.5	670	8.1 (4.8)	290.7	15
Mean		59.8	270.2	674	9.0 (5.3)	290.0	14
Standard Deviation		1.2	1.0	6	1.0 (0.5)	1.4	1

random pattern. Over land the two satellite analyses use similar thresholds and agree better. The agreement between the ISCCP and surface observations is excellent over the marine stratus regimes, suggesting that the smaller ISCCP threshold is more appropriate. However, this agreement may include some cancellation of two errors: an underestimate of cloud cover caused by the finite threshold (some cloudiness detected in the VIS data exhibits IR contrasts less than 2.5 K with clear ocean) and an overestimate of cloud amount caused by low resolution data (cf., Coakley and Bretherton 1982). The comparison of the surface observations and ISCCP over land suggests that the ISCCP results may be too low by about 5%. Disagreements among these climatologies are larger in the polar regions.

A third validation issue concerns just how well the radiative model and the two retrieved cloud properties (optical thickness and top temperature) represent the radiation field in a cloudy atmosphere (cf., Rossow and Lacis 1990). This involves not only checking the representation of the narrow-band radiances used in the analysis model, but also whether the same parameters and model can represent the full angular and spectral dependence of the radiation field. A crucial test of these parameters can be made by comparing

a calculated radiation budget using ISCCP to the measurements made by ERBE (e.g., Ramanathan et al. 1989).

b. Global time mean

The global annual mean cloud amount over three years is about 60%, the average optical thickness is about 9 (equivalent to a spherical albedo at 0.6 μm of about 50%), and the average cloud top temperature is 270 K (cloud top pressure is about 670 mb) (Table 3). Older climatologies had suggested mean cloud amounts of about 50% (see Hughes 1984) and some newer satellite-based analyses obtained similar results (Stowe et al. 1989; Rossow et al. 1989b); however, the lower values of the former appear to be caused by incomplete global coverage, especially of southern oceans, and of the latter by less sensitive detection procedures (cf., Fig. 6). The newer ground-based cloud climatology reports a global mean cloud amount of about 63% (Warren et al. 1986, 1988). Plate 1 shows the geographic distribution of cloud amount obtained by ISCCP, averaged over the period July 1983−June 1985. The classical climate zones are apparent in the variations of cloud amount. The midlatitude ocean storm track and the Intertropical Convergence Zone are associated with large cloud amounts exceeding 70%. Subtropical deserts are associated with cloud amounts below 40%. Some regions of subtropical oceans, particularly in the eastern Pacific, exhibit cloud amounts significantly less than 50%; however, the marine stratus regimes are indicated by cloud amounts > 60% off the west coasts of continents. The Antarctic plateau is much less cloudy than the Arctic basin (though polar results are less certain).

Average cloud top heights have been estimated in earlier analyses, indicating global annual mean values of 4−5 km (Henderson-Sellers 1986; Stowe et al. 1989; Rossow and Lacis 1990). The ISCCP cloud top pressure is equivalent to a mean altitude of about 3.5 km; however, detection of more low-level cloudiness, particularly over the oceans, accounts not only for the larger global mean cloud amount but also for the lower average cloud top altitude. Figure 8 shows the

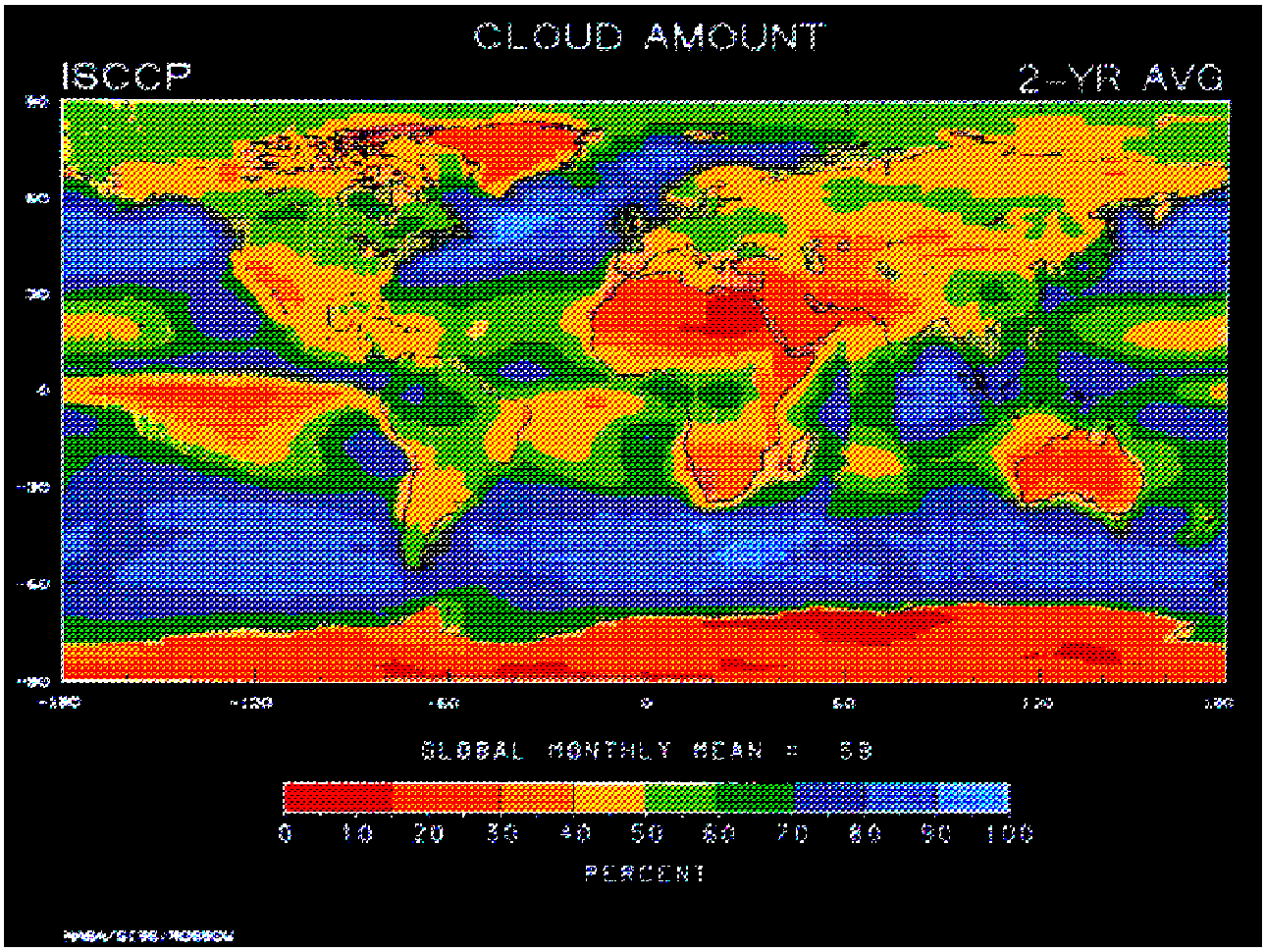

PLATE 1. Geographic distribution of cloud amount averaged over the first two years of ISCCP results: July 1983−June 1985. The color scale indicates cloud amount as percent of cloudy pixels found in the satellite images; the global mean value is also given.

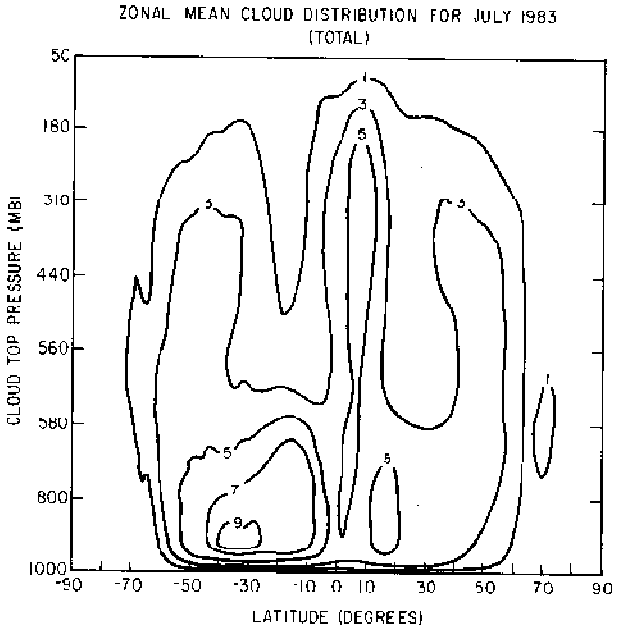

FIG. 8A

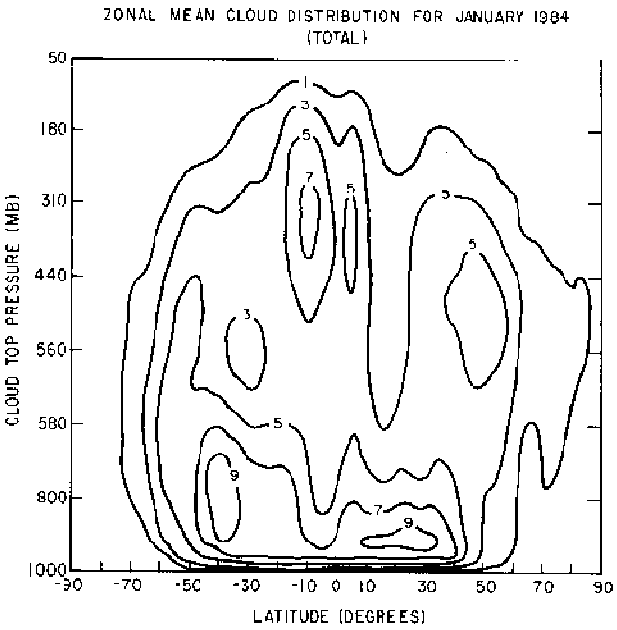

FIG. 8B

Frequency distribution of cloud top pressures collected over each latitude zone and month for (a) July 1983 and (b) January 1984. Contours indicate the proportion of total cloudiness with tops occurring in each pressure range (see Fig. 4) and latitude zone relative to the maximum (arbitrary) frequency of 10.

zonal mean cloud top pressure distribution for July 1983 and January 1984. The main climate regimes are revealed as a bimodal vertical distribution in the ITCZ, predominantly low-top clouds in the subtropics, and a more nearly uniform vertical distribution in middle latitudes. Middle latitude cloud tops are higher in winter than summer but do not extend as high as tropical clouds. The double ITCZ in January is less vertically developed than the narrower feature in July. Winter cloud tops over the North Pole occur at middle levels, while those over the South Pole occur at a very high altitude (not shown in Fig. 8a), consistent with the presence of Polar Stratospheric Clouds (Woodbury and McCormick 1986). This type of distribution information is provided at each location, every three hours in the Stage C1 data set.

The first direct determination from satellite data of cloud optical thickness and its regional variations was reported by Rossow et al. (1989b) and Rossow and Lacis (1990); however, earlier inferences suggested similar global mean values (e.g., Stephens 1984). The global annual mean value mentioned above is obtained by ordinary linear averaging, which gives more weight to larger values and provides better correspondence with estimates from cloud water contents. However, averaging in such a way as to give equal weight to clouds by their effect on the planetary albedo gives a global annual mean value of about 5 (equivalent to a spherical albedo at 0.6 μm of about 40%) (Table 3). The distribution of optical thicknesses for July 1983 and January 1984 is bi-modal in the ITCZ, with both a thick and a relatively thin component, is concentrated into a narrower range of moderate to thick optical thicknesses in the subtropics, and is more uniformly distributed over a larger range of values at midlatitudes. This type of distribution information is provided at each location, every three hours in the Stage C1 data set.

Various combinations of cloud top pressure and optical thickness define different "radiometric" cloud types (Fig. 4), but the geographic and seasonal distribution of these types appear consistent with the behavior of the classical cloud types that they are named after. Figure 9 shows two examples of the two-dimensional distribution of cloud properties collected over July 1983 and two particular latitude zones. In the subtropics in winter (Fig. 9a), the predominant cloud type has low tops and relatively low optical thickness (possibly associated with a highly broken nature), with the thicker clouds exhibiting somewhat higher tops: the relative proportion of cumulus and stratus suggested by Fig. 9a appears consistent with ground-based observations (Warren et al. 1986, 1988). The tropical cloud distribution, that exhibited a bi-modal distribution in cloud top pressure and optical thickness when considered separately, is shown to be tri-modal in Fig. 9b. The association of cumulus with the thinner, low-top cloud type, alto-

stratus and cirro-stratus with the moderate thickness, mid- to high-top cloud type (which is associated with meso-scale anvil structures in convective complexes), and deep convective towers with the thick, high-top cloud type is consistent with other evidence (Warren et al. 1986, 1988). The Intertropical Convergence Zone also has relatively large amounts of cirrus cloud (cf., Woodbury and McCormick 1986; Inoue 1989). This type of distribution information is provided at each location, every three hours in the Stage C1 data set.

c. Regional variations

Regional variations of the annual and monthly mean cloud and surface properties exhibit the well-known, complex patterns of the climate regimes. The cover figure illustrates this complexity on a particular day with a synthesized geostationary satellite view in IR over the Atlantic ocean with a spatial resolution of about 55 km. Regional variations in monthly mean cloud amounts, optical thicknesses and cloud top temperatures about their global averages are about 30%, about 10, and about 20 K, respectively. Surface temperatures vary by as much as 30 K, while surface reflectances vary by only about 10% in summer and by more than 50% in winter.

One major cause of regional cloud variability is the differences between clouds occurring over ocean and land. Figure 10 shows the distribution of 3-hourly cloud amounts for 280 km regions collected over the period July 1983−June 1984: there are more cloud-free regions over land and more completely overcast regions over oceans. Over oceans the distributions of cloud optical thickness and top pressure are shifted towards lower and higher values, respectively, indicating a predominance of low-level, broken cloudiness. Average cloud optical thicknesses over land are about 13, as contrasted with a value of about 9 for oceans;[6] cloud tops over land occur at about 4.5 km on average, as contrasted with a value of about 3.0 km over oceans. This difference is associated both with the differing mean altitudes of the land and ocean surface and with the generally higher cloud base heights over land (Warren et al. 1986, 1988).

d. Diurnal variations

Figure 11a illustrates the average diurnal variation of global mean cloudiness (here we use the cloud amount determined by IR-only for consistency) and surface temperature; the other parts of this figure show that this "complicated" global signal is produced by the summation of diurnal variations in different climate regimes with different amplitudes and phases. Over oceans the diurnal surface temperature vari-

[6]These values are obtained by linear averages and do not represent mean radiative affects.

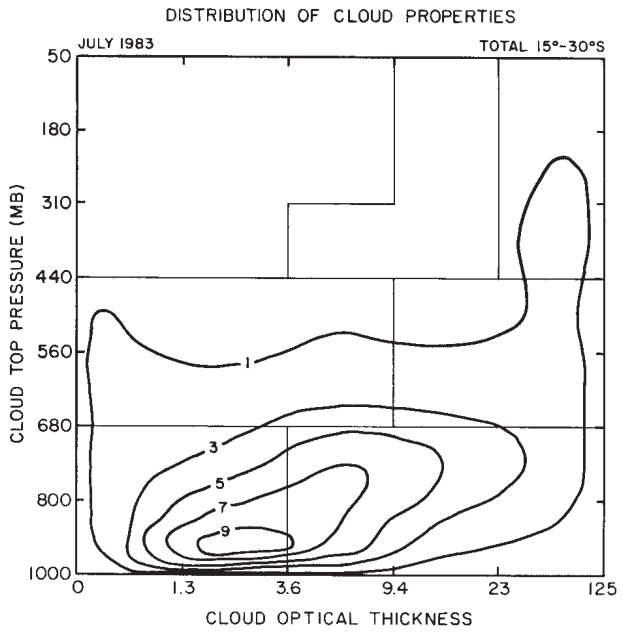

FIG. 9A

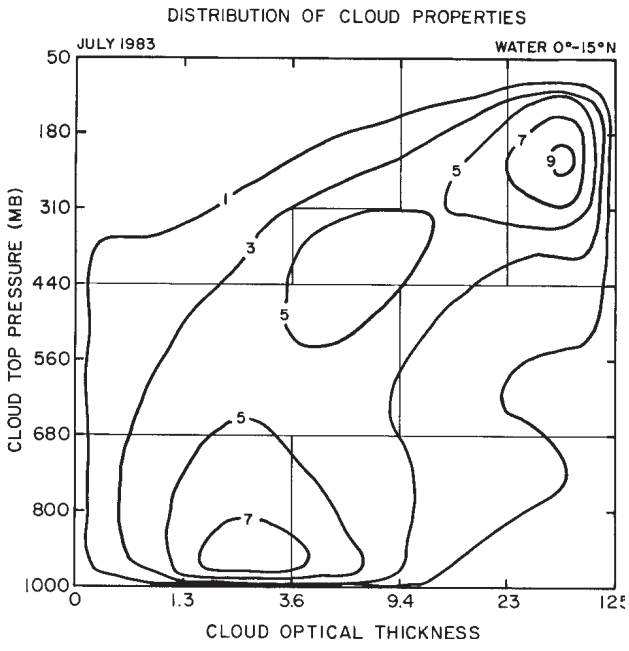

FIG. 9B

Frequency distribution of cloud optical thicknesses and cloud top pressures collected over July 1983 for a latitude zone in (a) the southern subtropics and (b) the northern tropics. Contours indicate the proportion of cloudiness in each cloud top pressure and optical thickness range relative to the (arbitrary) maximum amount of 10. Thin lines indicate the seven cloud types defined in Figure 4.

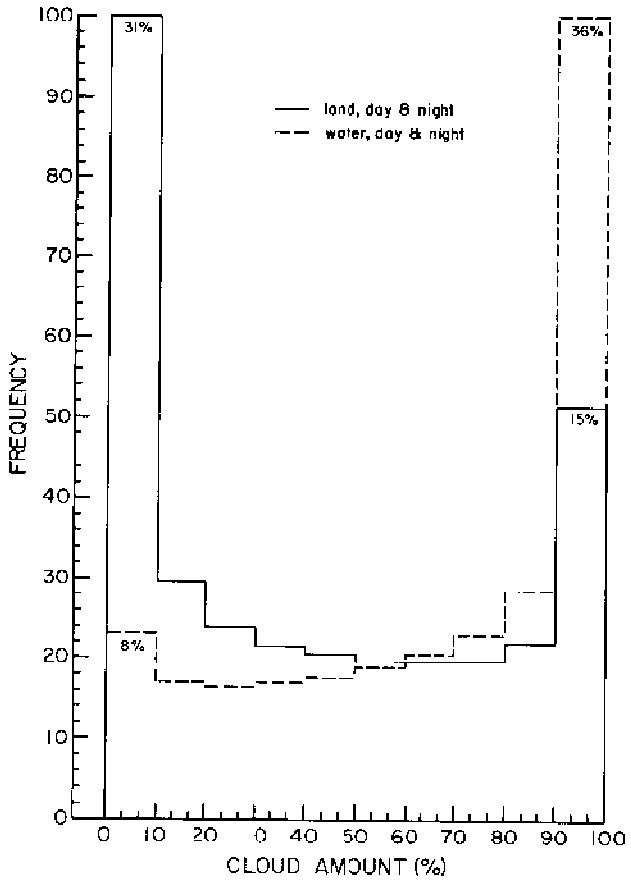

FIG. 10. Relative frequency distribution of cloud amount values occurring in 2.5° map grid cells every three hours for land (solid) and ocean (dashed) collected over the period July 1983−June 1984. Actual frequencies of cloud-free (< 10%) or completely overcast (≥ 90%) conditions over land and ocean are indicated.

ations are very small, with a maximum occurring in the mid-afternoon. Oceanic cloud amount variations are also small except at lower latitudes (Fig. 11b), where the maximum cloud amount occurs near dawn and the minimum occurs in the mid-afternoon (cf., Minnis and Harrison 1984). Diurnal variations of tropical convection show a phase lag of the mesoscale anvil clouds behind the convective towers (Fu et al. 1990). The diurnal variation of cloud amount over land at middle latitudes is very large in summer (Fig. 11c) and about half as great in winter; maximum cloud amount occurs in mid-afternoon, coincident with peak surface temperatures and convective activity, and the minimum occurs just after midnight with the lowest surface temperatures. However, diurnal variations are more complicated over tropical land areas (Fig. 11d): (1) the phase is reversed from midlatitudes with maximum cloud amount just after midnight and minimum cloud amount before noon, (2) there is a significant phase difference with the surface temperature, possibly indicating a large semi-diurnal component, and (3) there is significant regional variability of phase and amplitude. Stage C2 data provides this type of information about total cloudiness and ten cloud types at each location, each month.

e. Seasonal variations

Table 3 lists the global, monthly mean cloud and surface properties for the first three years of ISCCP analysis, July 1983 through June 1986. The amplitude of the global mean cloud and surface variations is much smaller than that observed at specific locations. The local range of seasonal cloud amounts, optical thicknesses and cloud top temperatures is about 30%, 10−20, and 20−30 K, respectively, although the regional variation of seasonal amplitudes is as large as the regional variation of mean properties about their global averages. These large seasonal variations at local scale nearly cancel in the global mean because of variations in both phase and amplitude. Figure 12 shows the resulting seasonal changes of global mean cloud amount and surface temperature. The "complex" behavior is produced by the summation of regional differences. For instance, the seasonal phases of the surface temperature variations of the northern and southern hemispheres are not exactly opposite and their amplitudes differ, because of differing land-ocean coverage. Similarly, the relation of cloud amount and cloud property variations to surface temperature varies from region to region, particularly from ocean to land. Tropical and mid-latitude variations are usually opposite in phase; tropical cloud amount variations dominate the seasonal changes of global mean cloud amount, while high latitude surface temperature variations dominate the seasonal changes of global mean surface temperature. Moreover, cloud amount, optical thickness and top temperature show different seasonal cycles. Hemispheric mean cloud amount is maximum in spring and fall and minimum in summer and winter. Hemispheric mean cloud optical thickness appears to be a maximum in spring and a minimum in winter; however, this may be caused (in part) by the changing proportion of midlatitude storm clouds that are illuminated by enough sunlight to measure their optical thickness. Summer and fall optical thicknesses are progressively lower than in spring. Hemispheric mean cloud top temperature varies together with surface temperature, because its variation is associated primarily with air temperature variations at higher latitudes; however, in the tropics the seasonal variations are caused by cloud top pressure variations that produce cloud top temperature variations that are anti-correlated with surface temperature.

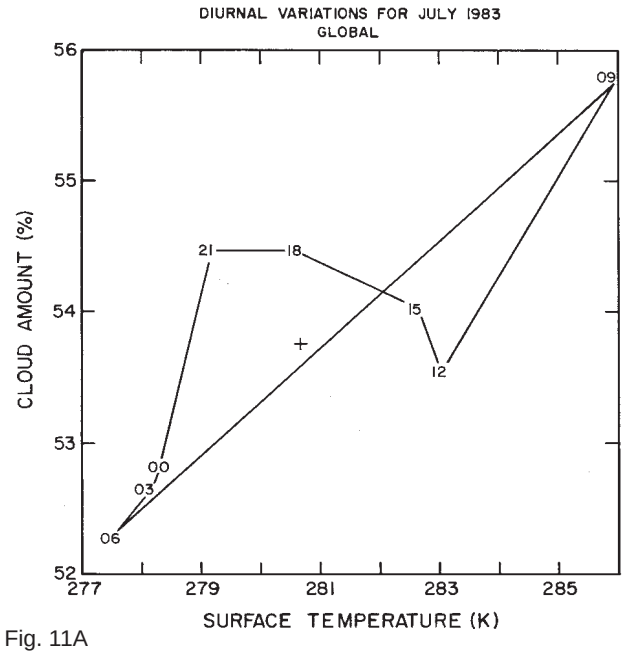

Fig. 11A

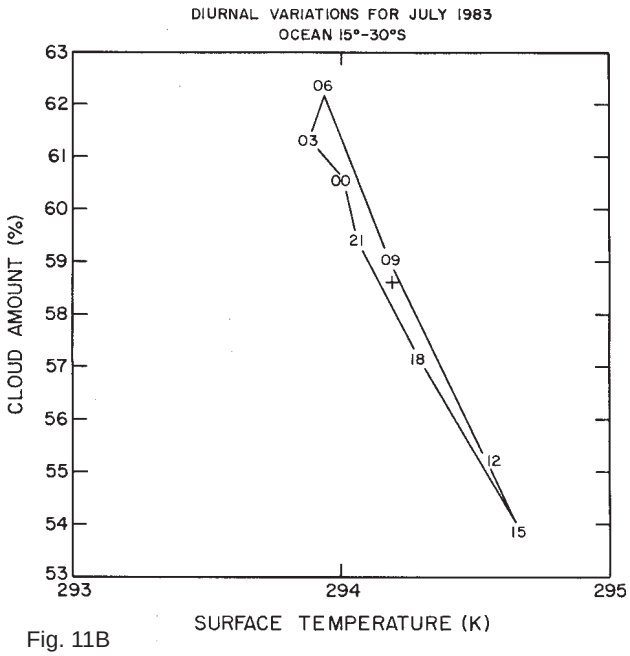

Fig. 11B

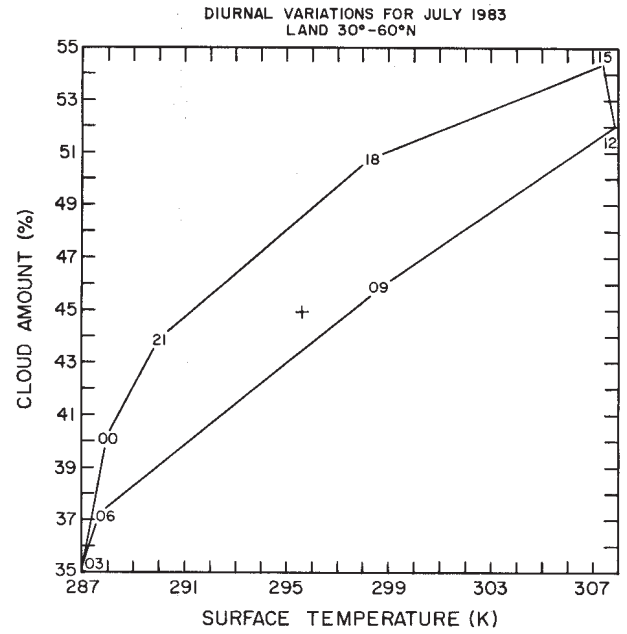

Fig. 11C

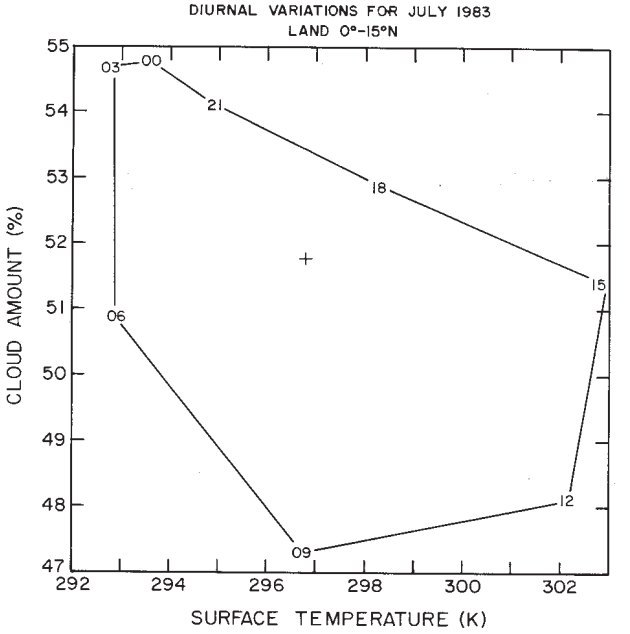

Fig. 11D

FIG. 11. Average diurnal variations of mean cloud amount versus mean surface temperature variations averaged over (a) the whole globe, (b) southern subtropical ocean areas, (c) northern midlatitude land areas, and (d) tropical land areas. Numbers indicate 3-hour intervals in local time, starting with midnight (=00). The + sign indicates the values averaged over the diurnal variations.

f. Interannual variations

Table 3 and Fig. 12 also illustrate how small the interannual variations of global mean values are, yet regional interannual variations are almost as large as their seasonal changes. The geographic patterns of the interannual changes show instances that can be explained by shifts in the location of otherwise constant cloud systems and instances where cloud amount and cloud properties have changed systematically. All of this complex regional variability appears to nearly cancel in global averages and produces slightly different seasonal cycles in different years (Fig. 12).

g. Implications

From the ISCCP results, the average albedo of the clouds is about twice the average albedo of the surface (the ratio is actually slightly smaller than at visible wavelengths because the land surface albedo is much higher at near-IR wavelengths), whereas the average temperature of the clouds is about midway between the average surface temperature and the effective radiating temperature of a clear, water-laden atmosphere. These relationships have been known qualitatively for a long time and suggest that the net effect of clouds on today's climate is a cooling (cf., Manabe and Strickler 1964). More direct inferences of the net cloud radiative effect shows that its quantitative magnitude is no more than 5-10% of the individual radiative flux components (Ramanathan et al. 1989), making accurate diagnosis very challenging.

Comparison of variations of cloud amount and properties on smaller space-time scales (meso-scale and daily) with those on larger scales (planetary and annual) shows that the former are much larger than the latter. The significant cancellation of these cloud variations when averaged over larger scales may suggest that the regional and short time variations can be thought of as perturbations of a quasi-equilibrium state by the motions of the atmosphere. However, year-to-year changes in the interactions among regions ("teleconnections") or in the precise summation of regionally varying amplitudes and phases do not produce the same seasonal variation of the global means and the same annual means every year (Fig. 12). This "statistical" effect could be a significant source of interannual variability in the climate.

A significant contributor to the differences in phase of seasonal variations appears to be different response time scales associated with dry land, "moist" or vegetated land, and ocean surface temperatures and their associated cloud types. Differing hemispheric distributions of cloud types associated with different distributions of surface types can explain much of the different seasonal behavior of the two hemispheres; differences in hemispheric behavior lead to more complex global behavior. Similar effects should appear in a transient climate change, where different parts of the system respond at different rates and the resulting changes can interact with each other to alter the regional response in unexpected ways. Consequently, the cloud-radiative feedbacks that may occur during a climate transition may be as complex as the seasonal ones.

The complex scale dependence and phase relations of the cloud variations have two important implications for studying and monitoring cloud processes in the climate. First, to isolate the simplest physical responses of clouds to changing environmental conditions requires sorting the observations to distinguish between different cloud types and different dynamic regimes. Although the cloud and surface/atmosphere variations may exhibit simple relationships locally, they do not add up to simple hemispheric or global variations. The possibility of representing cloud-climate feedbacks as simple functions of surface temperature, as in simple energy-balance climate models, or as a single global parameterization seems remote (cf., Rossow and Lacis 1990). Second, climate monitoring observations clearly must have sufficient time/space resolution to obtain an adequate statistical sample of all the significant scales of variation and must be complete in their coverage, since neglect of any portion of the diurnal cycle, synoptic variations, or the seasonal cycle, or neglect of any part of the globe can alias the monthly and annual statistics by amounts that might be larger than the magnitude of interannual changes and long-term trends.

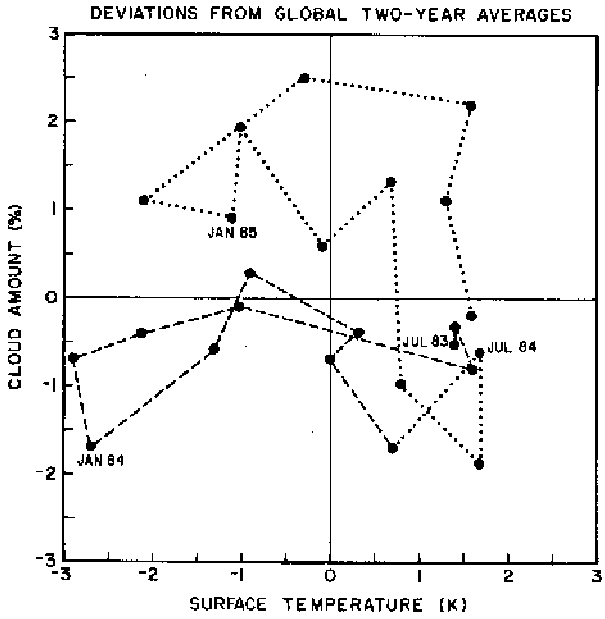

FIG. 12. Deviations of global, monthly mean cloud amounts and surface temperatures from their global, 2-year average values (July 1983 through June 1985). The line connects monthly values in sequence and changes from dashed to dotted at the end of the first year.

6. Project and data status

a. Radiance and correlative data

Production of Stage B3 radiance data is essentially routine; calibration and quality control activities generally require inspection of the data in a long-term context to detect slow drifts as well as shorter-term anomalies in radiometer performance. To date, Stage

B3 data have been delivered to the archives for the period July 1983 through December 1987. Data for 1988 should be completed by the end of 1990 and the backlog reduced to about one year by early 1991. Later in 1990 a special calibration and data quality data set will be produced to document the performance of all these satellite radiometers.

The special ISCCP versions of the TOVS atmospheric data and the combined snow and sea ice data set have been delivered for 1983 through 1989. Future deliveries will occur shortly after the end of each calendar year.

b. Cloud products

The Stage C1 and C2 cloud product data sets have been delivered covering the period from July 1983 through December 1986. On-going production is at a pace of about two years of data per calendar year; hence the first five years of the ISCCP cloud data should be available by mid-1991.

c. How to order data

All ISCCP data products are archived at NOAA/NESDIS:

Satellite Data Services Division (SDSD)
National Climatic Data Center (NCDC)
National Environmental Satellite Data and Information Service (NESDIS)
National Oceanic and Atmospheric Administration (NOAA)
Princeton Executive Square, Room 100
Washington, DC 20233, USA
Telephone: 301-763-8400
TELEX: RCA 248376 OBSWUR or TRT 197683 KWBC

A catalog of all ISCCP data sets is published by SDSD/NCDC/NESDIS/NOAA (WCRP 1988).

References

Arking, A., and J. D. Childs, 1985: Retrieval of cloud cover parameters from multispectral satellite measurements. *J. Climate Appl. Meteor.*, **24,** 322-333.

Barkstrom, B. R., and G. L. Smith, 1986: The Earth Radiation Budget Experiment: Science and implications. *Rev. Geophys.*, **2**, 379-390.

Brest, C.L., and W. B. Rossow, 1990: Radiometric calibration and monitoring of NOAA AVHRR data for ISCCP, *Int. J. Remote Sensing* (in press).

Coakley, J. A., and F. P. Bretherton, 1982: Cloud cover from high-resolution scanner data: Detecting and allowing for partially filled fields of view. *J. Geophys. Res.,* **87,** 4917-4932.

Cox, S. K., D. S. McDougal, D. A. Randall and R. A. Schiffer, 1987: FIRE − the First ISCCP Regional Experiment. *Bull. Amer. Meteor. Soc.,* **68,** 114-112.

Desbois, M., and G. Sèze, 1984: Use of space and time sampling to produce representative satellite cloud classifications. *Ann. Geophys.*, **2 (5),** 599-606.

Fu, R., A. D. Del Genio and W. B. Rossow, 1990: Behavior of deep convective clouds in the tropical Pacific deduced from ISCCP radiances. *J. Atmos. Sci.* (in press).

Gutman, G., D. Tarpley and G. Ohring, 1987: Cloud screening for determination of land surface characteristics in a reduced resolution satellite data set. *Int. J. Remote Sensing,* **8,** 859-870.

Henderson-Sellers, A. 1986: Layer cloud amounts for January and July 1979 from 3-D nephanalysis. *J. Climate Appl. Meteor.,* **25,** 118-132.

Hughes, N. A., 1984: Global cloud climatologies: A historical review. *J. Climate Appl. Meteor.*, **23,** 724-751.

Inoue, T., 1989: Features of clouds over the tropical Pacific during northern hemispheric winter derived from split window measurements. *J. Meteor. Soc. Japan*, **67**, 621-637.

Karl, T. R., J. D. Tarpley, R. G. Quayle, H. F. Diaz, D. A. Robinson and R. S. Bradley, 1989: The recent climate record: What it can and cannot tell us. *Rev. Geophys., 27,* 405-430.

Manabe, S., and R. F. Strickler, 1964: Thermal equilibrium of the atmosphere with a convective adjustment. *J. Atmos. Sci.* **21,** 361-385.

Minnis, P., and E. F. Harrison, 1984: Diurnal variability of regional cloud and clear sky radiative parameters derived from GOES data. Part II: November 1978 cloud distributions. *J. Climate Appl. Meteor.,* **23**, 1012-1031.

Oort, A.H., 1983: Global Atmospheric Circulation Statistics, 1958-1973. NOAA Professional Paper 14, NOAA Geophysical Fluid Dynamics Laboratory, U.S. Dept. of Commerce, Rockville, MD, 180 pp.

Ramanathan, V., R. D. Cess, E. F. Harrison, P. Minnis, B. R. Barkstrom, E. Ahmad and D. Hartmann, 1989: Cloud-radiative forcing and climate: Results from the Earth Radiation Budget Experiment. *Science*, **243**, 57-63.

Reynolds, R. W., 1988: A real-time global sea surface temperature analysis. *J. Climate,* **1,** 75-86.

Rossow, W. B., 1989: Measuring cloud properties from space: A review. *J. Climate*, **2,** 201-213.

Rossow, W. B., and L. C. Garder, 1984: Selection of a map grid for data analysis and archival. *J. Climate Appl. Meteor.,* **23,** 1253-1257.

Rossow, W. B., and A. A. Lacis, 1990: Global, seasonal cloud variations from satellite radiance measurements. Part II: Cloud properties and radiative effects. *J. Climate* (in press).

Rossow, W. B., F. Mosher, E. Kinsella, A. Arking, M. Desbois, E. Harrison, P. Minnis, E. Ruprecht, G. Sèze, C. Simmer and E. Smith, 1985: ISCCP cloud algorithm intercomparison. *J. Climate Appl. Meteor.*, **24**, 877-903.

Rossow, W. B., E. Kinsella, and A. Wolf, 1987: International Satellite Cloud Climatology project (ISCCP) Description of Reduced Resolution Radiance Data. July 1985 (revised July 1987). WMO/TD-No. 58, World Meteorological Organization, Geneva, 143 pp.

Rossow, W. B., L. C. Garder, P. J. Lu and A. W. Walker 1988: International Satellite Cloud Climatology Project (ISCCP) Documentation of Cloud Data. WMO/TD-No. 266, World Meteorological Organization, Geneva, 78 pp. plus two appendices.

Rossow, W. B., C. L. Brest, and L. C. Garder, 1989a: Global, seasonal surface variations from satellite radiance measurements. *J. Climate*, **2,** 214-247.

Rossow, W. B., L. C. Garder, and A. A. Lacis, 1989b: Global, seasonal cloud variations from satellite radiance measurements. Part I: Sensitivity of analysis. *J. Climate*, **2,** 419-458.

Schiffer, R. A., and W. B. Rossow, 1983: The International Satellite Cloud Climatology Project (ISCCP): The first project of the World Climate Research Program. *Bull. Amer. Meteor. Soc.*, **64**, 779-784.

Schiffer, R. A., and W. B. Rossow, 1985: ISCCP global radiance data set: A new resource for climate research. *Bull. Amer. Meteor. Soc.*, **66**, 1498-1505.

Schluessel, P., H-Y. Shin, W. J. Emery and H. Grassl, 1987: Comparison of satellite-derived sea surface temperatures with in situ measurements. *J. Geophys. Res.*, **92,** 2859-2874.

Sèze, G., and M. Desbois, 1987: Cloud cover analysis from satellite imagery using spatial and temporal characteristics of the data. *J. Climate Appl. Meteor.*, **26**, 287-303.

Sèze, G., and W. B. Rossow, 1990: Time-cumulated visible and infrared radiance histograms used as descriptors of surface and cloud variations. *Int. J. Remote Sensing* (in press).

Stephens, G. L., 1984: The parameterization of radiation for numerical weather prediction and climate models. *Mon. Wea. Rev.,* **112,** 826-867.

Stephens, G. L., 1988: Radiative transfer through arbitrarily shaped optical media, II: Group theory and simple closures. *J. Atmos. Sci*., **45,** 1837-1848.

Stowe, L. L., C. G. Wellemeyer, T. F. Eck, H. Y. M. Yeh and the NIMBUS-7 Cloud Data Processing Team, 1988: Nimbus-7 global cloud climatology. Part I: Algorithms and validation. *J. Climate,* **1**, 445-470.

Stowe, L. L., C. G. Wellemeyer, T. F. Eck, H. Y. M. Yeh and the NIMBUS-7 Cloud Data Processing Team, 1989: Nimbus-7 global cloud climatology. Part II. *J. Climate*, **2,** 641-655.

Warren, S. G., C. J. Hahn and J. London, 1985: Simultaneous occurrence of different cloud types. *J. Climate Appl. Meteor.*, **24,** 658-667.

Warren, S. G., C. J. Hahn, J. London, R. M. Chervin and R. L. Jenne, 1986: Global distribution of total cloud cover and cloud type amounts over land. NCAR Technical Note NCAR/TN-273 + STR, National Center for Atmospheric Research, Boulder, CO (also DOE/ER/60085-H1).

Warren, S. G., C. J. Hahn, J. London, R. M. Chervin, and R. L. Jenne, 1988: Global distribution of total cloud cover and cloud type amounts over ocean. NCAR Technical Note NCAR/TN-317 + STR, National Center for Atmospheric Research, Boulder, CO, 42 pp. plus 170 maps.

WCP 1985: Report of the Workshop on Global Large-Scale Precipitation Data Sets for the WCRP, Camp Springs, Maryland, 24-25 July 1985. WCP-111, World Meteorological Organization, Geneva.

WCP, 1986a: The International Satellite Cloud Climatology Project (ISCCP) Research Plan and Validation Strategy, January 1986, WMO/TD-No. 88. World Meteorological Organization, Geneva.

WCP, 1986b: Report of the Workshop on Surface Radiation Budget for Climate Applications, Columbia, Maryland, 18-21 June 1985. WCP-115, World Meteorological Organization, Geneva, 144 pp.

WCP, 1987: Report of the Workshop on Space Systems Possibilities for a Global Energy and Water Cycle Experiment, Columbia Maryland, 19-23 January 1987. WCP-137, World Meteorological Organization, Geneva, 38 pp. plus 11 appendices.

WCRP, 1984a: *Scientific Plan for the World Climate Research Programme.* WCRP Publ. Series, No. 2, WMO/TD-No. 6, World Meteorological Organization, Geneva, 95 pp.

WCRP, 1984b: *Development of the Implementation Plan for the International Satellite Land-Surface Climatology Project (ISLSCP) Phase I.* H-J. Bolle and S. I. Rasool, Eds., WMO/TD 46, World Meteorological Organization, Geneva, 89 pp.

WCRP, 1988: International Satellite Cloud Climatology Project (ISCCP) Catalog of Data and Products, Dec. 1988 (rev. Oct. 1989). K. B. Kidwell and B. J. Worthington, Eds., WMO/TD-NO. 265.

Whitlock, C. H.. W. F. Staylor, G. Smith, R. Levin, R. Frouin, C. Gautier, P. M. Teillet, P. N. Slater, Y. J. Kaufman, B. N. Holben, W. B. Rossow, C. L. Brest and S.R. LeCroy, 1990: AVHRR and VISSR satellite instrument calibration results for both cirrus and marine stratocumulus IFO periods. FIRE Science Report 1988. NASA CP-3083 (in press).

WMO, 1989: Report of the Tenth Session of the Joint Scientific Committee, Villefranche-sur-mer, France, 13-18 March 1989. WMO/RD-No. 314, World Meteorological Organization, Geneva, 57 pp. plus 3 appendices.

Woodbury, G. E., and M. P. McCormick, 1986: Zonal and geographic distributions on cirrus clouds determined from SAGE data. *J. Geophys. Res.,* **91**, 2775-2785.

Wright, P., 1986: Problems in the use of ship observations for the study of interdecadal climate changes. *Mon. Wea. Rev.* **114,** 1028-1034.